Inorg. Chem. **2002**, *41*, 4923–4935

Factors Influencing Conformer Equilibria in Retro Models of Cisplatin–DNA Adducts As Revealed by Moderately Dynamic (*N,N′*-Dimethyl-2,3-diaminobutane)PtG_2 Retro Models (G = a Guanine Derivative)

Jamil S. Saad,[†] Tommaso Scarcia,[‡] Giovanni Natile,*[,‡] and Luigi G. Marzilli*[,†,||]

Department of Chemistry, Emory University, Atlanta, Georgia 30322, and Dipartimento Farmaco-Chimico, Università di Bari, Via E. Orabona 4, 70125 Bari, Italy

Received October 29, 2001

Typical *cis*-PtA_2**G**$_2$ models of key DNA lesions formed by cis-type Pt anticancer drugs are very dynamic and difficult to characterize (A_2 = diamine or two amines; **G** = guanine derivative). Retro models have A_2 carrier ligands designed to decrease dynamic motion without eliminating any of three possible conformers with bases oriented head-to-tail (two: ΔHT and ΛHT) or head-to-head (one: HH). *All three* were found in NMR studies of eight **Me$_2$DAB**Pt**G**$_2$ retro models (**Me$_2$DAB** = *N,N′*-dimethyl-2,3-diaminobutane with *S,R,R,S* and *R,S,S,R* configurations at the chelate ring N, C, C, and N atoms, respectively; **G** = 5′-GMP, 3′-GMP, 5′-IMP, and 3′-IMP). The bases cant to the left (L) in (*S,R,R,S*)-**Me$_2$DAB**Pt**G**$_2$ adducts and to the right (R) in (*R,S,S,R*)-**Me$_2$DAB**Pt**G**$_2$ adducts. Relative to the case in which the bases are both not canted, canting will move the six-membered rings closer in to each other ("6-in" form) or farther out from each other ("6-out" form). Interligand interactions between ligand components near to Pt (first-first sphere communication = FFC) or far from Pt (second-sphere communication = SSC) influence stability. In typical cases at pH < 8, the "6-in" form is favored, although the larger six-membered rings of the bases are close. In minor "6-out" HT forms, the proximity of the smaller five-membered rings could be sterically favorable. Also, **G** O6 is closer to the sterically less demanding NH part of the **Me$_2$DAB** ligand, possibly allowing **G** O6–NH hydrogen bonding. These favorable FFC effects do not fully compensate for possibly stronger FFC dipole effects in the "6-in" form. SSC, phosphate–N1H cis **G** interactions favor ΛHT forms in 5′-GMP and 5′-IMP complexes and ΔHT forms in 3′-GMP and 3′-IMP complexes. When SSC and FFC favor the same HT conformer, it is present at >90% abundance. In six adducts [four (*S,R,R,S*)-**Me$_2$DAB**Pt**G**$_2$ and (*R,S,S,R*)-**Me$_2$DAB**Pt**G**$_2$ (**G** = 3′-GMP and 3′-IMP)], the minor "6-out" HT form at pH ∼7 becomes the major form at pH ∼10, where **G** N1H is deprotonated, because the large distance between the negatively charged N1 atoms minimizes electrostatic repulsion and probably because the **G** O6–(NH)**Me$_2$DAB** H-bond (FFC) is strengthened by N1H deprotonation. At pH ∼10, phosphate-negative N1 repulsion is an unfavorable SSC term. This factor disfavors the ΛHT R form of two (*R,S,S,R*)-**Me$_2$DAB**Pt**G**$_2$ (**G** = 5′-GMP and 5′-IMP) adducts to such an extent that the "6-in" ΔHT R form remains the dominant form even at pH ∼10.

Introduction

Platinum complexes and their interactions with nucleotides and nucleic acids have been studied extensively over the last 30 years.[1] Interest in such interactions stems from the discovery that cisplatin (*cis*-Pt$(NH_3)_2Cl_2$) shows exceptional activity against testicular and ovarian cancers and increasing promise against head/neck tumors.[2−5] To date, more than 3000 platinum compounds have been prepared and tested in attempts to improve the cytostatic activity and reduce the toxicity of cisplatin or its analogue, carboplatin;[6,7] about 30 of these compounds have entered clinical trials.[8] The intrastrand N7−Pt−N7 cross-link between two adjacent G

* To whom correspondence should be addressed. E-mail: lmarzil@lsu.edu.
[†] Emory University.
[‡] Università di Bari.
[||] New address: Chemistry Department, Louisiana State University, Baton Rouge, LA 70803.

(1) *Cisplatin: Chemistry and Biochemistry of a Leading Anticancer Drug*; Lippert, B., Ed.; Wiley-VCH: Weinheim, Germany, 1999.

10.1021/ic011115m CCC: $22.00
Published on Web 08/22/2002

residues leading to a DNA distortion is widely accepted as being the critical biomolecular interaction leading to a DNA distortion responsible for the activity of cis-type platinum anticancer drugs.[6,7,9−11]

Many Pt compounds form these cross-link adducts, but few have good activity approaching that of cisplatin. Thus, secondary factors arising from the carrier ligand are important in influencing activity. *cis*-PtA_2X_2 agents (A_2 = two amines or a diamine carrier ligand; X = leaving group) have lower or no activity when no NH groups are present.[6,7] Hydrogen bonding between bound G ligands and the two Pt−NH_3 groups of cisplatin has been an important component of hypotheses concerning factors stabilizing the distortions in DNA induced by the intrastrand lesion.[7,12−17] However, distances in an X-ray/NMR-derived model of a duplex 9-oligomer[11] and an X-ray structure of an HMG-bound 16-oligomer,[18] both containing the intrastrand cisplatin lesion with a similar structure, suggest that such hydrogen-bonding interactions involving the Pt−NH_3 groups are at best weak. Furthermore, when the two NH_3 ligands are replaced by A_2 carrier ligands having sp^3 N's bearing two or more alkyl groups in computer models of these duplex structures, unfavorable clashes result.[11] In fact, carrier ligand−DNA H-bonds are also absent in the crystal structure of a cisplatin interstrand adduct in which G bases in the Pt−DNA adduct adopt a ΔHT conformation.[19] These and other observations led us to hypothesize[11,20] that the very small size of the NH group, not its hydrogen-bonding ability, is responsible for the good activity exhibited by Pt compounds with amine carrier ligands bearing multiple NH groups. Although we propose that the solution structure of duplexes is essentially solved,[11] the duplex structure contains considerably more

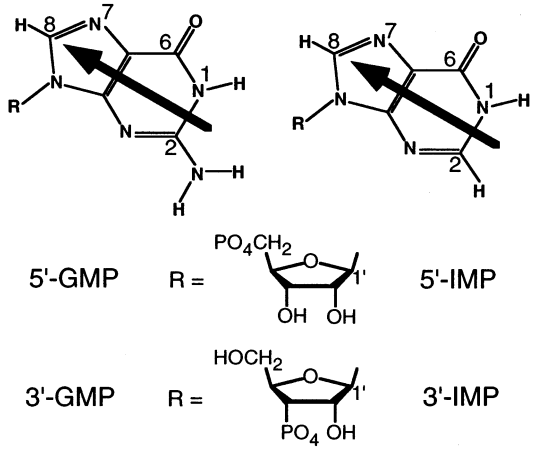

Figure 1. Guanine (left) and inosine (right) derivatives. (The arrow and its head represent the base and the H8 atom, respectively.)

DNA distortion and less Pt geometry distortion than previously suggested. Thus, controversy still exists.[21] Also, although the focus has been on duplexes, at the physiologically relevant 37 °C, considerable "DNA breathing" is likely near Pt−DNA lesions, as suggested by NMR data[10] and a study involving reagents that react only with single-strand regions.[22] Unusual conformers having single-strand character and affecting anticancer activity or repair mechanisms probably exist at 37 °C. Indeed, a DNA hairpin containing the cis-coordinated G(N7)−Pt−G(N7) intrastrand cross-link was shown to have a unique head-to-side conformation.[23] Finally, other "non-cis" classes of Pt compounds exhibit activity associated with forming adducts at G in DNA.[24−27] Thus exploring the fundamental chemistry of Pt-G adducts has broad relevance.

To gain a better understanding of a number of fundamental factors influencing properties of Pt−G adducts, we need to know the effect of the carrier ligand interactions with the nucleic acid constituents (the bases, sugars, etc.). These interactions, present in very small adducts, are also present in larger models including duplexes. However, they can be more difficult to assess in the larger adducts, particularly because larger adducts manifest additional interactions involving both flanking residues in the cross-link strand and residues in the complementary strand.

In this report we focus on *cis*-$PtA_2\mathbf{G}_2$ models (**G** = N9-substituted guanine derivative (Figure 1); the bold letter indicates a guanine not linked to another guanine). Bases can have head-to-tail (HT) or head-to-head (HH) conformers. For *cis*-$PtA_2\mathbf{G}_2$, cross-link models with C_2-symmetrical carrier ligands have one HH and two HT (ΔHT and ΛHT)

(2) O'Dwyer, P. J.; Stevenson, J. P.; Johnson, S. W. In *Cisplatin: Chemistry and Biochemistry of a Leading Anticancer Drug*; Lippert, B., Ed.; Wiley-VCH: Weinheim, Germany, 1999; pp 31−72.
(3) O'Dwyer, P. J.; Stevenson, J. P.; Johnson, S. W. *Drugs* **2000**, *59*, 19−27.
(4) Rosenberg, B. In *Cisplatin: Chemistry and Biochemistry of a Leading Anticancer Drug*; Lippert, B., Ed.; Wiley-VCH: Weinheim, Germany, 1999; pp 3−30.
(5) Wong, E.; Giandomenico, C. M. *Chem. Rev.* **1999**, *99*, 2451−2466.
(6) Hambley, T. W. *Coord. Chem. Rev.* **1997**, *166*, 181−223.
(7) Jamieson, E. R.; Lippard, S. J. *Chem. Rev.* **1999**, *99*, 2467−2498.
(8) Lebwohl, D.; Canetta, R. *Eur. J. Cancer* **1998**, *34*, 1522−1534.
(9) Reedijk, J. *Chem. Commun.* **1996**, 801−806.
(10) Ano, S. O.; Kuklenyik, Z.; Marzilli, L. G. In *Cisplatin: Chemistry and Biochemistry of a Leading Anticancer Drug*; Lippert, B., Ed.; Wiley-VCH: Weinheim, Germany, 1999; pp 247−291.
(11) Marzilli, L. G.; Saad, J. S.; Kuklenyik, Z.; Keating, K. A.; Xu, Y. *J. Am. Chem. Soc.* **2001**, *123*, 2764−2770.
(12) van Garderen, C. J.; Bloemink, M. J.; Richardson, E.; Reedijk, J. *J. Inorg. Biochem.* **1991**, *42*, 199−205.
(13) Reedijk, J. *Inorg. Chim. Acta* **1992**, *198−200*, 873−881.
(14) Sherman, S. E.; Gibson, D.; Wang, A.; Lippard, S. J. *J. Am. Chem. Soc.* **1988**, *110*, 7368−7381.
(15) Farrell, N. In *Metal Ions in Biological Systems*; Sigel, A., Sigel, H., Eds.; Marcel Dekker: New York, 1996; Vol. 32, pp 603−639.
(16) Laoui, A.; Kozelka, J.; Chottard, J.-C. *Inorg. Chem.* **1988**, *27*, 2751−2753.
(17) Bloemink, M. J.; Heetebrij, R. J.; Inagaki, K.; Kidani, Y.; Reedijk, J. *Inorg. Chem.* **1992**, *31*, 4656−4661.
(18) Ohndorf, U.-M.; Rould, M. A.; He, Q.; Pabo, C. O.; Lippard, S. J. *Nature* **1999**, *399*, 708−712.
(19) Coste, F.; Malinge, J.-M.; Serre, L.; Shepard, W.; Roth, M.; Leng, M.; Zelwer, C. *Nucleic Acids Res.* **1999**, *27*, 1837−1846.
(20) Sullivan, S. T.; Ciccarese, A.; Fanizzi, F. P.; Marzilli, L. G. *J. Am. Chem. Soc.* **2001**, *123*, 9345−9355.
(21) Hambley, T. W. *J. Chem. Soc., Dalton Trans.* **2001**, 2711−2718.
(22) Malina, J.; Hofr, C.; Maresca, L.; Natile, G.; Brabec, V. *Biophys. J.* **2000**, *78*, 2008−2021.
(23) Iwamoto, M.; Mukundan, S., Jr.; Marzilli, L. G. *J. Am. Chem. Soc.* **1994**, *116*, 6238−6244.
(24) Zakovska, A.; Novakova, O.; Balcarova, Z.; Bierbach, U.; Farrell, N.; Brabec, V. *Eur. J. Biochem.* **1998**, *254*, 547−557.
(25) Bierbach, U.; Farrell, N. *J. Biol. Inorg. Chem.* **1998**, *6*, 570−580.
(26) Bierbach, U.; Qu, Y.; Hambley, T. W.; Peroutka, J.; Nguyen, H. L.; Doedee, M.; Farrell, N. *Inorg. Chem.* **1999**, *38*, 3535−3542.
(27) Brabec, V.; Neplechova, K.; Kasparkova, J.; Farrell, N. *J. Biol. Inorg. Chem.* **2000**, *5*, 364−368.

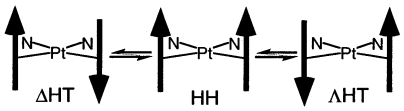

Figure 2. Shorthand representation of ΛHT, ΔHT, and HH conformations with the carrier ligand to the rear. Arrows represent the **G** bases with **G** H8 near the tip and the **G** O6 near the blunt end.

conformers (Figure 2). Conformer interconversion requires rotation about one or both Pt−N7 bonds. In most cisplatin adducts, this rotation is fast on the NMR time scale, making it impossible to use NMR methods to assess which forms are present. We refer to this and other problems in applying NMR methods in the typical way as the "dynamic motion problem".[20,28−39] Even in large adducts, which are generally accepted to be mainly HH, multiple conformations in fast exchange on the NMR scale with one dominant conformation cannot be ruled out.[10] Duplex models have most recently been studied in solution at low temperature (∼5 °C), where breathing is minimal.[10,11]

The "dynamic motion problem" led us to construct analogues of cisplatin with bulky ligands designed to reduce the dynamic motion by destabilizing the transition state for Pt−N7 rotation. An important feature of the design is to minimize steric effects of the ground state equilibrium species to allow conformers likely to be present in dynamic *cis*-$PtA_2\mathbf{G}_2$ adducts to exist in the new adducts also. We have introduced the term "retro-modeling"[30] to emphasize that the models we employ[20,28−31,33−39] are more complicated than the relevant molecule, cisplatin. By reducing rotation rates by a billionfold,[28,30] retro models have enabled us to understand the adducts of the highly fluxional cisplatin drug with DNA constituents.[37] Retro-model results[20,28−32,35,36,38,39] place in doubt the following two concepts, which until recently were widely accepted from studies on dynamic platinum complexes: (i) The untethered **G**'s adopt a HT conformation in preference to the HH conformation.[10] (ii) Single-stranded d(GpG) cross-links favor the HH form, which undergoes slow Pt−G N7 bond rotation.[40−44]

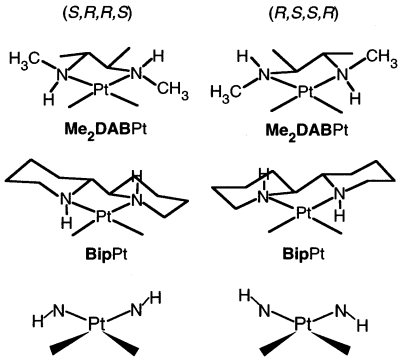

Figure 3. Sketches of the **Bip**Pt and **Me$_2$DAB**Pt moieties.

Me$_2$DAB (*N*,*N*′-dimethyl-2,3-diaminobutane) was the carrier ligand in the first such detailed NMR retro-model study.[31,45,46] *(Note that we designate diamine carrier ligands in boldface type.)* **Me$_2$DAB** is one of the chirality-controlling chelates (CCC) having chiral centers on the amines and the chelate ring carbons. Most of our work involves the C_2-symmetrical *S*,*R*,*R*,*S* and *R*,*S*,*S*,*R* isomers, in which the chiral centers are the N, C, C, and N chelate ring atoms, respectively (Figure 3). The **Me$_2$DAB** retro models provided the opportunity to define the solution structure of conformers by NMR methods allowing us to identify the HH form of a *cis*-$PtA_2\mathbf{G}_2$ adduct for the first time[45] and to define the absolute conformation in solution.[31] In addition to **Me$_2$DAB** compounds, we have studied **en** (**en** = ethylenediamine), **Bip** (2,2′-bipiperidine), another **CCC** ligand (Figure 3), **Me$_2$ppz** (*N*,*N*′-dimethylpiperazine), **Me$_2$DAP** (*N*,*N*′-dimethyl-2,4-diaminopentane), and **pipen** (2-(aminomethyl)piperidine).[28,30,31,33−36,39,45,47] The atropisomerization rate depends on the amine ligand as follows: $(NH_3)_2 \sim$ **en** > **Me$_2$DAP** > **Me$_2$DAB** ≫ **pipen** > **Me$_2$ppz** ∼ **Bip**.

The **Me$_2$DAB** ligand occupies a central position in the series. The **Me$_2$DAB**Pt$\mathbf{G}_2$ conformers interchanged too rapidly to permit HPLC separation.[31] This problem led us to design the more rigid bicyclic **Bip CCC** ligand (Figure 3). **Bip**Pt$\mathbf{G}_2$ adducts can be separated by HPLC and converted to nonequilibrium metastable states useful for studying larger adducts.[29] At high pH, **Bip**Pt$\mathbf{G}_2$ adducts were difficult to study for two reasons: First, the long time needed for equilibrium to be reached (> 1 day) made it difficult to construct a complete profile of conformer distribution vs pH. Second, as **Bip**Pt$\mathbf{G}_2$ adducts approached equilibrium, H8 H/D exchange would occur, making it impossible to probe changes in conformer distribution and H8 shifts with the H8 signals. Thus, we return here to the NMR study of the more

(28) Ano, S. O.; Intini, F. P.; Natile, G.; Marzilli, L. G. *J. Am. Chem. Soc.* **1997**, *119*, 8570−8571.
(29) Ano, S. O.; Intini, F. P.; Natile, G.; Marzilli, L. G. *J. Am. Chem. Soc.* **1998**, *120*, 12017−12022.
(30) Ano, S. O.; Intini, F. P.; Natile, G.; Marzilli, L. G. *Inorg. Chem.* **1999**, *38*, 2989−2999.
(31) Marzilli, L. G.; Intini, F. P.; Kiser, D.; Wong, H. C.; Ano, S. O.; Marzilli, P. A.; Natile, G. *Inorg. Chem.* **1998**, *37*, 6898−6905.
(32) Marzilli, L. G.; Ano, S. O.; Intini, F. P.; Natile, G. *J. Am. Chem. Soc.* **1999**, *121*, 9133−9142.
(33) Wong, H. C.; Intini, F. P.; Natile, G.; Marzilli, L. G. *Inorg. Chem.* **1999**, *38*, 1006−1014.
(34) Wong, H. C.; Coogan, R.; Intini, F. P.; Natile, G.; Marzilli, L. G. *Inorg. Chem.* **1999**, *38*, 777−787.
(35) Sullivan, S. T.; Ciccarese, A.; Fanizzi, F. P.; Marzilli, L. G. *Inorg. Chem.* **2000**, *39*, 836−842.
(36) Sullivan, S. T.; Ciccarese, A.; Fanizzi, F. P.; Marzilli, L. G. *Inorg. Chem.* **2001**, *40*, 455−462.
(37) Wong, H. C.; Shinozuka, K.; Natile, G.; Marzilli, L. G. *Inorg. Chim. Acta* **2000**, *297*, 36−46.
(38) Williams, K. M.; Cerasino, L.; Natile, G.; Marzilli, L. G. *J. Am. Chem. Soc.* **2000**, *122*, 8021−8030.
(39) Saad, J. S.; Scarcia, T.; Shinozuka, K.; Natile, G.; Marzilli, L. G. *Inorg. Chem.* **2002**, *41*, 546−557.
(40) den Hartog, J. H. J.; Altona, C.; Chottard, J.-C.; Girault, J.-P.; Lallemand, J.-Y.; de Leeuw, F. A. A. M.; Marcelis, A. T. M.; Reedijk, J. *Nucleic Acids Res.* **1982**, *10*, 4715−4730.
(41) Girault, J.-P.; Chottard, G.; Lallemand, J.-Y.; Chottard, J.-C. *Biochemistry* **1982**, *21*, 1352−1356.
(42) Kozelka, J.; Fouchet, M.-H.; Chottard, J.-C. *Eur. J. Biochem.* **1992**, *205*, 895−906.
(43) Neumann, J.-M.; Tran-Dinh, S.; Girault, J.-P.; Chottard, J.-C.; Huynh-Dinh, T. *Eur. J. Biochem.* **1984**, *141*, 465−472.
(44) Berners-Price, S. J.; Ranford, J. D.; Sadler, P. J. *Inorg. Chem.* **1994**, *33*, 5842−5846.
(45) Xu, Y.; Natile, G.; Intini, F. P.; Marzilli, L. G. *J. Am. Chem. Soc.* **1990**, *112*, 8177−8179.
(46) Kiser, D.; Intini, F. P.; Xu, Y. H.; Natile, G.; Marzilli, L. G. *Inorg. Chem.* **1994**, *33*, 4149−4158.
(47) Williams, K. M.; Cerasino, L.; Intini, F. P.; Natile, G.; Marzilli, L. G. *Inorg. Chem.* **1998**, *37*, 5260−5268.

Table 1. H8 Chemical Shifts (ppm) of **Me$_2$DAB**Pt(3′-GMP)$_2$ and **Me$_2$DAB**Pt(5′-GMP)$_2$ Complexes at Different pH Values

complex	pH	ΛHT	ΔHT	HH_u	HH_d
(*S*,*R*,*R*,*S*)-**Me$_2$DAB**Pt(3′-GMP)$_2$	3.4[a]	8.45	8.31	8.03	8.81
	7.2[a]	8.48	8.55	8.03	8.83
	9.6[a]	8.42	7.79	7.53	8.75
(*R*,*S*,*S*,*R*)-**Me$_2$DAB**Pt(3′-GMP)$_2$	3.3	8.26	8.55	*b*	*b*
	6.9	8.27	8.57	*b*	*b*
	9.3	8.01	8.45	*b*	*b*
(*S*,*R*,*R*,*S*)-**Me$_2$DAB**Pt(5′-GMP)$_2$	3.2	8.54	8.28	8.01	8.95
	7.1	8.54	8.30	8.01	9.19
	10.4	8.50	8.04	7.54	9.07
(*R*,*S*,*S*,*R*)-**Me$_2$DAB**Pt(5′-GMP)$_2$	3.1	8.27	8.73	8.09	8.95
	7.3	8.37	8.88	8.14	9.22
	10.0	8.15	8.81	7.72	9.15

[a] At 5 °C; all others were at room temperature. [b] Not determined.

convenient, moderately dynamic **Me$_2$DAB**Pt**G**$_2$ models with **G** = 5′-GMP, 3′-GMP, 5′-IMP, and 3′-IMP in the pH range of ∼3 to ∼10, to examine more fully factors influencing conformation of *cis*-PtA$_2$**G**$_2$ adducts. IMP's lack the 2-NH_2 group of GMP's (Figure 1), allowing us to assess the effect of the 2-NH_2 group. The present fundamental study focuses on the HT forms, which now appear to be possible also in longer single-strand adducts.[48]

Experimental Section

Materials. 5′-GMP, 3′-GMP, 5′-IMP, and 3′-IMP (Sigma) were used as received. Preparation of the (*S*,*R*,*R*,*S*)-**Me$_2$DAB**Pt(SO_4)(H_2O) and (*R*,*S*,*S*,*R*)-**Me$_2$DAB**Pt(SO_4)(H_2O) complexes has been described elsewhere.[45]

Methods. A typical preparation of bis adducts involved treatment of ∼2 equiv of **G** with 1 equiv (∼10 mM) of **Me$_2$DAB**Pt(SO_4)(H_2O) in D_2O (0.6 mL) at pH ∼3. Reactions were monitored by ^{1}H NMR spectroscopy until either no free **G** H8 signal or no change in H8 signal intensity was observed. Standard DNO_3 and NaOD solutions (in D_2O) were used for adjusting the pH (uncorrected) of the samples directly in the NMR tubes when needed.

1D ^{1}H NMR spectra, obtained on a GE GN-Omega 600 spectrometer, were referenced to the residual HOD peak. In a typical experiment, a selective presaturation pulse (30 dB) was applied for 2 s to the residual HOD resonance. The FID was accumulated for 32 transients in blocks containing 16K data points. Before Fourier transformation, the FID's were baseline corrected for dc offset, and then an exponential multiplication apodization function with a 0.2 Hz line broadening was applied. To change the sample pH, a small drop of either DNO_3 or NaOD solution was added directly to the NMR tube. NMR spectra were recorded at increments of ∼0.3 to 0.5 pH units from pH ∼3 to pH ∼10. NMR studies were performed at 25 °C and, in those cases in which observation of the HH and HT NMR signals required lower temperatures, at 5 °C.

Results

At pH ∼3, **Me$_2$DAB**Pt(5′-GMP)$_2$ and **Me$_2$DAB**Pt(3′-GMP)$_2$ complexes have four H8 signals previously assigned to the HH, ΔHT, and ΛHT conformers (the HH conformer has two nonequivalent **G**'s, giving HH_u (upfield HH) and HH_d (downfield HH) signals) (Table 1).[31,45] For **Me$_2$DAB**-Pt(5′-IMP)$_2$ and **Me$_2$DAB**Pt(3′-IMP)$_2$ complexes at pH ∼3, the analogous conformers were obtained, but the presence of the H2 signal doubled (to eight) the number of aromatic singlets (Table 2). From their relative intensities, the H2 signals (usually upfield of the H8 signals) are easily assigned to a given conformer. Shifts of the ^{1}H NMR signals of the GMP and IMP ligands provide probes of the structural features. For IMP adducts, the H2 atom is on the opposite end of the base from H8 (schematically, on the tail of the arrow, Figure 2). The plane of the bases generally is not perpendicular to the coordination plane, and the canting can be either left-handed (L) or right-handed (R), Figure 4. Canting places either the H2 or the H8 of a given base close to the shielding cone of the cis **G**. The H2 signal follows the opposite trend as the H8 signal. For clarity, the H2 NMR signals are labeled as HH_c (canted HH base, H8 upfield, H2 downfield) and HH_n (not so canted base, H8 downfield, H2 upfield). An analogous interpretation of the consequence of this head/tail relationship on the ^{1}H NMR signals of protons on different rings of lopsided ligands has been offered for Ru(II) and Re(V) trimethylbenzimidazole complexes.[49−53] This explanation can also be applied to Ru(II) complexes with other ligands[54−56] and to Pt−1-Me-5′-GMP adducts.[39]

pH Studies. For all **Me$_2$DAB**Pt**G**$_2$ adducts, conformers equilibrated quickly, making it feasible to follow the pH dependence at small pH steps. Two relevant types of ionizable groups are present in the general *cis*-PtA$_2$(GMP)$_2$ type of adducts studied here. First, the monoanionic $ROPO_3D^-$ ligands below pH 4 become fully deprotonated by pH ∼7.5.[57−61] The lower phosphate group pK_a of 5.6 to 6.2 vs 6.3 for free 5′-GMP[30,34,47,60,62,63] has been attributed either to H-bonding between the phosphate group and the amine hydrogen[44,64,65] or to the electrostatic effect of the positively charged platinum.[66] Second, the **G** N1H groups deprotonate with pK_a values of 8.7 and ∼9.4 for *cis*-PtA$_2$(5′-GMP)$_2$ vs

(48) Sullivan, S. T.; Saad, J. S.; Fanizzi, F. P.; Marzilli, L. G. *J. Am. Chem. Soc.* **2002**, *124*, 1558−1559.

(49) Marzilli, L. G.; Iwamoto, M.; Alessio, E.; Hansen, L.; Calligaris, M. *J. Am. Chem. Soc.* **1994**, *116*, 815−816.
(50) Alessio, E.; Calligaris, M.; Iwamoto, M.; Marzilli, L. G. *Inorg. Chem.* **1996**, *35*, 2538−2545.
(51) Alessio, E.; Hansen, L.; Iwamoto, M.; Marzilli, L. G. *J. Am. Chem. Soc.* **1996**, *118*, 7593−7600.
(52) Marzilli, L. G.; Marzilli, P. A.; Alessio, E. *Pure Appl. Chem.* **1998**, *70*, 961−968.
(53) Alessio, E.; Zangrando, E.; Iengo, E.; Macchi, M.; Marzilli, P. A.; Marzilli, L. G. *Inorg. Chem.* **2000**, *39*, 294−303.
(54) Iwamoto, M.; Alessio, E.; Marzilli, L. G. *Inorg. Chem.* **1996**, *35*, 2384−2389.
(55) Alessio, E.; Zangrando, E.; Roppa, R.; Marzilli, L. G. *Inorg. Chem.* **1998**, *37*, 2458−2463.
(56) Velders, A. H.; Hotze, A. C. G.; van Albada, G. A.; Haasnoot, J. G.; Reedijk, J. *Inorg. Chem.* **2000**, *39*, 4073−4080.
(57) Lippert, B. *Prog. Inorg. Chem.* **1989**, *37*, 1−97.
(58) Martin, R. B. *Acc. Chem. Res.* **1985**, *18*, 32−38.
(59) Johnson, N. P.; Butour, J.-L.; Villani, G.; Wimmer, F. L.; Defais, M.; Pierson, V.; Brabec, V. *Prog. Clin. Biochem. Med.* **1989**, *10*, 1−24.
(60) Sigel, H.; Massoud, S. S.; Corfù, N. A. *J. Am. Chem. Soc.* **1994**, *116*, 2958−2971.
(61) Sigel, H.; Lippert, B. *Pure Appl. Chem.* **1998**, *70*, 845−854.
(62) Saenger, W. *Principles of Nucleic Acid Structure*; Springer-Verlag: New York, 1984; pp 1−556.
(63) Song, B.; Zhao, J.; Griesser, R.; Meiser, C.; Sigel, H.; Lippert, B. *Chem.−Eur. J.* **1999**, *5*, 2374−2387.
(64) Berners-Price, S. J.; Frey, U.; Ranford, J. D.; Sadler, P. J. *J. Am. Chem. Soc.* **1993**, *115*, 8649−8659.
(65) Reily, M.; Marzilli, L. G. *J. Am. Chem. Soc.* **1986**, *108*, 6785−6793.
(66) Song, B.; Oswald, G.; Bastian, M.; Sigel, H.; Lippert, B. *Metal-Based Drugs* **1999**, *3*, 131−141.

Table 2. H8 and (in Parentheses) H2 Shifts (ppm) for **Me$_2$DAB**Pt(3′-IMP)$_2$ and **Me$_2$DAB**Pt(5′-IMP)$_2$ Complexes

complex	pH	ΛHT	ΔHT	HH_u (HH_c)	HH_d (HH_n)
(*S*,*R*,*R*,*S*)-**Me$_2$DAB**Pt(3′-IMP)$_2$	3.3[a]	8.88 (8.22)	8.80 (8.28)	8.49 (8.30)	9.23 (8.16)
	7.0[a]	8.89 (8.21)	8.90 (8.26)	8.43 (8.30)	9.25 (8.16)
	9.8[a]	8.78 (8.11)	8.31 (8.26)	8.15 (8.11)	9.09 (8.02)
(*R*,*S*,*S*,*R*)-**Me$_2$DAB**Pt(3′-IMP)$_2$	3.0	8.71 (8.30)	8.98 (8.16)	*b*	*b*
	7.3	8.58 (8.27)	9.00 (8.09)	*b*	*b*
	9.6	8.32 (8.23)	8.69 (8.09)	*b*	*b*
(*S*,*R*,*R*,*S*)-**Me$_2$DAB**Pt(5′-IMP)$_2$	3.3	9.00 (8.17)	8.71 (8.29)	8.51 (*b*)	9.36 (8.13)
	7.0	9.03 (8.17)	8.73 (8.28)	8.48 (*b*)	9.60 (8.13)
	10.4	8.92 (8.02)	8.42 (8.24)	7.84 (*b*)	9.43 (*b*)
(*R*,*S*,*S*,*R*)-**Me$_2$DAB**Pt(5′-IMP)$_2$	3.5	8.65 (8.32)	9.21 (8.15)	8.56 (8.32)	9.38 (8.18)
	7.2	8.76 (8.30)	9.39 (8.11)	8.62 (8.29)	9.62 (8.16)
	10.1	8.47 (*b*)	9.22 (7.94)	8.23 (8.20)	9.47 (8.06)

[a] At 5 °C; all others were at room temperature. [b] Not determined because of overlap.

Figure 4. Shorthand representation of left-handed and right-handed canting.

9.5 for free 5′-GMP.[60,61,63] The lower N1H pK_a values of Pt**G**$_2$ adducts are due to the inductive effects of the Pt bound to N7. [41,60,63,67] In NMP's (NMP = nucleotide monophosphate), because of the electrostatic effect of the negatively charged phosphate groups and the different position of 3′ relative to 5′ groups from the base, the pK_a value of N1H increases by ∼0.5 unit when going from nucleoside to 3′-NMP to 5′-NMP.[62] For both the phosphate and N1H groups, the pK_a values of free 5′-IMP and 5′-GMP are very similar;[58] thus, the 2-NH_2 group in 5′-GMP has little effect.

For all **Me$_2$DAB**Pt**G**$_2$ adducts studied here, we show in Supporting Information plots of the H8 shifts vs pH for all observed conformers. Between pH ∼7.5 and pH ∼10, N1H deprotonation is typically detected by upfield-shifting of the H8 signal.[30,33,57−59,68,69] The study of N1H deprotonation effects on distribution was complicated by some isomerization of the asymmetric N centers in the **Me$_2$DAB** ligand when the pH was raised above ∼9.5. Isomerization was detected by the appearance of additional small ^{1}H NMR signals. These signals were still observed after the pH was dropped from a high value to ∼4.

***(S,R,R,S)*-Me$_2$DABPt(3′-GMP)$_2$.** The four H8 signals for (*S*,*R*,*R*,*S*)-**Me$_2$DAB**Pt(3′-GMP)$_2$ at pH ∼3 and 5 °C were assigned[31] to the ΛHT (major), ΔHT, and HH conformers (Figure 5). Of these signals, only the ΔHT H8 signal shifted significantly (downfield by 0.24 ppm) when the pH was raised to ∼7 (Table 1). This change due to phosphate deprotonation was accompanied by an increase in the abundance of the ΔHT conformer (Figures 5 and 6). At pH >8, all four H8 signals shifted upfield, marking the N1H deprotonation; the conformer distribution changed greatly, with the ΔHT conformer clearly dominant at pH 9.6 (Table 3).

***(S,R,R,S)*-Me$_2$DABPt(3′-IMP)$_2$.** The four H8 signals observed for (*S*,*R*,*R*,*S*)-**Me$_2$DAB**Pt(3′-IMP)$_2$ at pH ∼3 and 5 °C (Figure 7) were assigned by analogy to (*S*,*R*,*R*,*S*)-**Me$_2$DAB**Pt(3′-GMP)$_2$, while the signals of their H2 partners were assigned on the basis of signal intensities. The H8 and H2 signals of the ΛHT conformer are more downfield and upfield, respectively, than for the ΔHT conformer (Table 2). From pH ∼3 to ∼7, the ΔHT H8 signal shifted downfield by 0.1 ppm (this signal shifted downfield by 0.2 ppm at pH 6.5, Supporting Information); the ΛHT H8 and HH_d signals shifted only slightly downfield (∼0.02 ppm), and the HH_u signal shifted upfield by 0.06 ppm. None of the H2 signals shifted downfield when the phosphate group was deprotonated. At pH 9.8, all H8 signals shifted upfield by 0.2 to 0.6 ppm; furthermore, the ΛHT H2, HH_c, and HH_n signals shifted upfield by 0.1−0.2 ppm, while the ΔHT H2 signal did not shift.

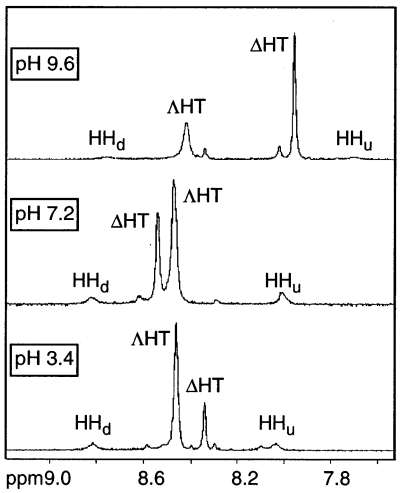

Figure 5. H8 ^{1}H NMR signals of (*S*,*R*,*R*,*S*)-**Me$_2$DAB**Pt(3′-GMP)$_2$ at different pH values and 5 °C. Unlabeled small peaks arise from carrier ligand isomerization or slight impurities.

The distribution of (*S*,*R*,*R*,*S*)-**Me$_2$DAB**Pt(3′-IMP)$_2$ conformers vs pH (Table 3 and Supporting Information) was very similar to that of (*S*,*R*,*R*,*S*)-**Me$_2$DAB**Pt(3′-GMP)$_2$ (Figure 6 and Table 3). The ΛHT conformer dominates when the phosphate groups are protonated (below pH 5). From pH ∼5 to pH ∼7.5, an increase in the ΔHT conformer population results from phosphate deprotonation. As N1H deprotonation begins (pH ∼7.5), the ΛHT:ΔHT ratio changes; at pH ∼8 it is inverted, and by pH 9.8 the ΔHT conformer is dominant.

(67) Chu, G. Y. H.; Mansy, S.; Duncan, R. E.; Tobias, R. S. *J. Am. Chem. Soc.* **1978**, *100*, 593−606.
(68) den Hartog, J. H. J.; Altona, C.; van der Marel, G. A.; Reedijk, J. *Eur. J. Biochem.* **1985**, *147*, 371−379.
(69) Elizondo-Riojas, M.-A.; Kozelka, J. *Inorg. Chim. Acta* **2000**, *297*, 417−420.

Table 3. Conformer Percentages of **Me$_2$DAB**Pt**G**$_2$ Complexes at Different pH Values Measured from the H8 Signal Intensities

	(*S*,*R*,*R*,*S*)				(*R*,*S*,*S*,*R*)			
G	pH	% ΛHT	% ΔHT	% HH	pH	% ΛHT	% ΔHT	% HH
3′-GMP	3.4[a]	80	13	7	3.3	16	84	*b*
	7.2[a]	60	35	5	6.9	4	96	*b*
	9.6[a]	37	60	3	9.3	86	14	*b*
3′-IMP	3.3[a]	72	17	11	3.0	13	87	*b*
	7.0[a]	63	30	7	7.3	5	95	*b*
	9.8[a]	41	56	3	9.6	83	17	*b*
5′-GMP	3.2	92	2	6	3.1	7	71	22
	7.0	98	1	1	7.3	12	70	18
	10.4	20	72	8	10.0	10	69	21
5′-IMP	3.3	90	2	8	3.5	6	72	22
	7.1	97	1	2	7.2	4	77	19
	10.4	16	70	14	10.1	2	79	19

[a] At 5 °C; all others were at room temperature. [b] Not determined.

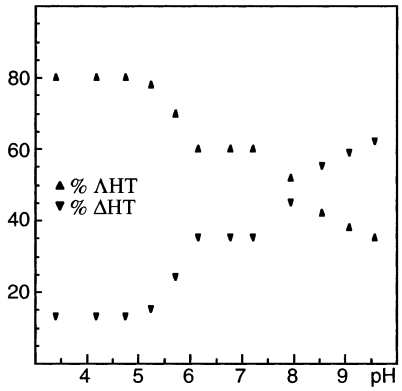

Figure 6. Population distribution of the ΛHT and ΔHT conformers of (*S*,*R*,*R*,*S*)-**Me$_2$DAB**Pt(3′-GMP)$_2$ as a function of pH. The HH distribution was not included in the plot because it did not change significantly.

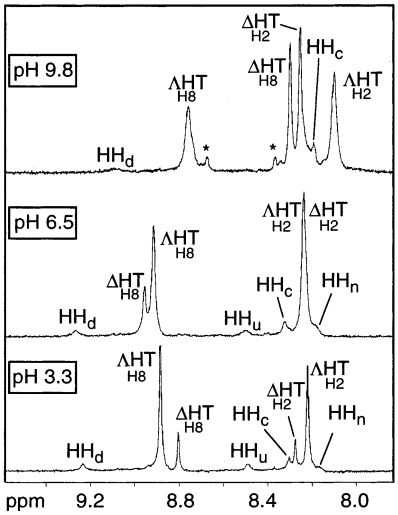

Figure 7. H8 and H2 ^{1}H NMR signals of (*S*,*R*,*R*,*S*)-**Me$_2$DAB**Pt(3′-IMP)$_2$ at different pH values and 5 °C. The asterisks indicate compounds with isomerized **Me$_2$DAB**.

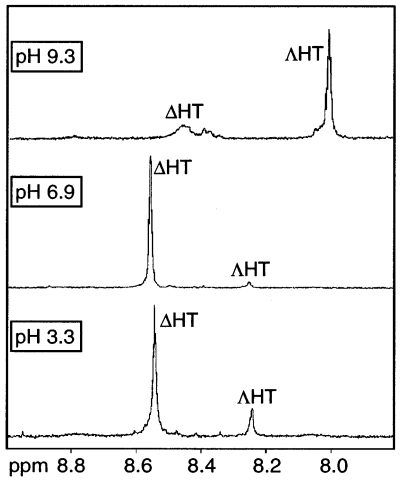

Figure 8. H8 ^{1}H NMR signals of (*R*,*S*,*S*,*R*)-**Me$_2$DAB**Pt(3′-GMP)$_2$ at different pH values and 25 °C. The HH peaks are not labeled in the spectra because they are barely visible.

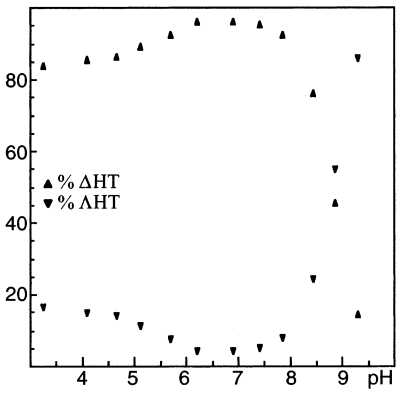

Figure 9. Distribution of the ΔHT and ΛHT conformers of (*R*,*S*,*S*,*R*)-**Me$_2$DAB**Pt(3′-GMP)$_2$ as a function of pH. The HH distribution (not included) did not change significantly.

(*R*,*S*,*S*,*R*)-Me$_2$DABPt(3′-GMP)$_2$. At pH ∼3 and 25 °C, the two H8 signals observed (Figure 8) were assigned[31] to the ΔHT (major) and ΛHT conformers, whereas the H8 signals of the HH conformer were not detectable because the conformer interconversion rate was fast enough to broaden the signals of this minor conformer. The HH$_u$ and HH$_d$ signals are visible in the ^{1}H NMR spectrum of (*R*,*S*,*S*,*R*)-**Bip**Pt(3′-GMP)$_2$,[30] which exhibits a lesser degree of dynamic motion. On increase of the pH to 6.9 (phosphate deprotonation), the ΔHT and ΛHT H8 signals shifted slightly downfield (Table 1) and the favored ΔHT conformer became highly dominant (Table 3). At pH 9.3 (N1 H deprotonated), both the ΛHT and the ΔHT H8 signals shifted upfield by 0.10−0.25 ppm and the ΛHT conformer was highly dominant (Figures 8 and 9).

(*R*,*S*,*S*,*R*)-Me$_2$DABPt(3′-IMP)$_2$. For (*R*,*S*,*S*,*R*)-**Me$_2$DAB**-Pt(3′-IMP)$_2$, the four ^{1}H NMR signals observed at pH ∼3

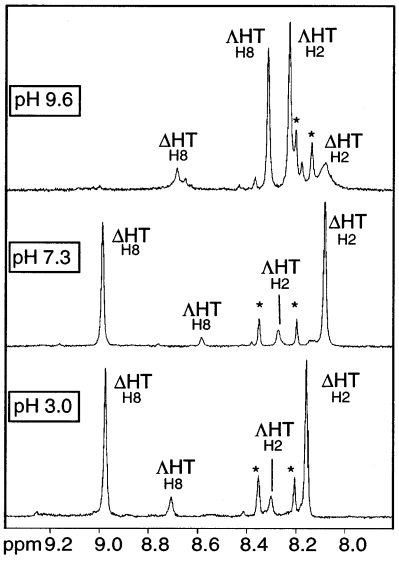

Figure 10. H8 and H2 ^{1}H NMR signals of (*R,S,S,R*)-**Me$_2$DAB**Pt(3′-IMP)$_2$ at different pH values and 25 °C. The HH peaks are not labeled because these are barely visible. Asterisks mark free 3′-IMP. Unlabeled small peaks arise from compounds with isomerized **Me$_2$DAB**.

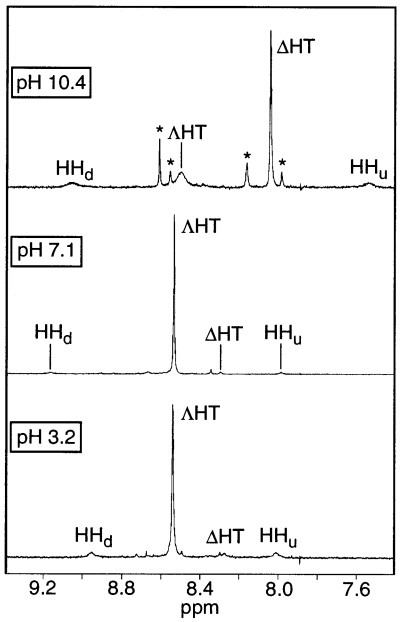

Figure 11. H8 ^{1}H NMR signals of (*S,R,R,S*)-**Me$_2$DAB**Pt(5′-GMP)$_2$ at different pH values and 25 °C. Asterisks indicate peaks arising from compounds with isomerized **Me$_2$DAB**.

and 25 °C are assigned to the H8 and H2 resonances of the ΔHT and ΛHT conformers (Figure 10). The HH signals were broad for reasons given above. The H8 and H2 signals of the ΔHT conformer are more downfield and upfield than for the minor ΛHT conformer (Table 2). In the range from pH ∼5 to pH ∼8, phosphate deprotonation causes shift changes (Table 3). The N1H deprotonation leads to an upfield shift for both the ΛHT and ΔHT H8 signals; a slight shift occurred for the ΛHT H2 signal, while the ΔHT H2 signal did not shift (Table 2). The conformer profile was very similar for both (*R,S,S,R*)-**Me$_2$DAB**Pt(3′-GMP)$_2$ and (*R,S,S,R*)-**Me$_2$DAB**Pt(3′-IMP)$_2$ (Figure 9 and Supporting Information). For both adducts, the highly dominant ΔHT conformer at pH ∼3 becomes more favored upon phosphate deprotonation (∼95%), but in the pH range 8.5−9.0 (where N1H deprotonation becomes significant) the ΛHT form became dominant.

***(S,R,R,S)*-Me$_2$DABPt(5′-GMP)$_2$.** The four H8 signals of (*S,R,R,S*)-**Me$_2$DAB**Pt(5′-GMP)$_2$ were assigned[31] to the ΛHT (major), ΔHT, and HH conformers (Figure 11). From pH ∼3 to pH ∼7 (phosphate deprotonation), the HH$_d$ signal shifted significantly downfield by 0.24 ppm; ΔHT H8 signals shifted slightly downfield by ∼0.02 ppm, while HH$_u$ and ΛHT H8 signals did not shift (Table 1). Furthermore, the population of the HH form dropped significantly (Table 3); the ΛHT conformer became so dominant (∼98%) that the signals of the other two conformers were barely visible. As the pH was increased from ∼7 to ∼10 (N1H deprotonation), all H8 signals shifted upfield (Table 1) and the ΔHT conformer became highly dominant (Figure 11 and Table 3).

***(S,R,R,S)*-Me$_2$DABPt(5′-IMP)$_2$.** For (*S,R,R,S*)-**Me$_2$DAB**-Pt(5′-IMP)$_2$ at pH ∼3, the four H8 and four H2 signals (Supporting Information) are assigned to the ΛHT (major), ΔHT, and HH conformers. Each H8 NMR signal was assigned by analogy to (*S,R,R,S*)-**Me$_2$DAB**Pt(5′-GMP)$_2$. As the pH was increased from ∼3 to ∼7, some of the H8 signals shifted downfield (Table 2). The HH$_d$ signal experienced the largest shift change (0.24 ppm), while the ΛHT and ΔHT H8 signals shifted slightly downfield; the HH$_u$ signal shifted slightly upfield. Furthermore, at pH ∼7 the ΛHT conformer became highly dominant (97%). As the pH was increased from ∼7 to ∼10, all H8 signals of the HH and HT conformers shifted upfield (Table 2). At pH 10.4, the ΔHT conformer displaced the ΛHT form as the highly dominant form (Supporting Information). In contrast to the 3′-NMP adducts, a higher pH (∼10 vs ∼9) was needed to invert the ΛHT/ΔHT ratio for (*S,R,R,S*)-**Me$_2$DAB**Pt(5′-GMP)$_2$ and the respective 5′-IMP adduct (Table 3 and Supporting Information). This result is consistent with the higher N1H pK_a value for 5′-NMP's compared to the 3′-NMP's.[62]

***(R,S,S,R)*-Me$_2$DABPt(5′-GMP)$_2$.** The four H8 signals of (*R,S,S,R*)-**Me$_2$DAB**Pt(5′-GMP)$_2$ at pH ∼3 and 25 °C are indicative of the typical three conformers, the major form being the ΔHT conformer (Figure 12).[45] In the pH range of ∼3 to ∼7, all H8 signals shifted downfield (Table 1). At pH ∼7, the intensity of both the ΔHT and HH H8 signals decreased, while the intensity of the ΛHT H8 signal increased (Figure 12). Between pH ∼7 and pH ∼10, all H8 signals shifted upfield and the conformer distribution changed only slightly (Table 3). The ΔHT conformer was highly dominant at pH 10.0.

***(R,S,S,R)*-Me$_2$DABPt(5′-IMP)$_2$.** The four H8/H2 pairs of signals of (*R,S,S,R*)-**Me$_2$DAB**Pt(5′-IMP)$_2$ at pH ∼3 (Supporting Information) were assigned on the basis of the (*R,S,S,R*)-**Me$_2$DAB**Pt(5′-GMP)$_2$ results. The ΔHT form dominated. From pH ∼3 to pH ∼7, all H8 signals shifted downfield (Table 2) and the intensity of signals changed only slightly. From pH ∼7 to pH ∼10, all H8 signals shifted upfield (Table 2 and Supporting Information); only slight changes occurred in the intensity of the signals. At pH 10.1,

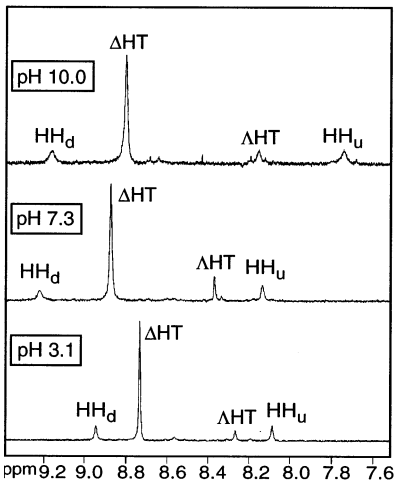

Figure 12. H8 ^{1}H NMR signals of (*R*,*S*,*S*,*R*)-**Me$_2$DAB**Pt(5′-GMP)$_2$ at different pH values and 25 °C. Unlabeled small peaks arise from compounds with isomerized **Me$_2$DAB**.

the ΔHT conformer was still highly dominant. This behavior was similar to that of the analogous 5′-GMP adducts. *These two* (*R*,*S*,*S*,*R*)-***Me$_2$DAB****Pt(5′-NMP)$_2$ adducts are anomalous because the same form dominated at both high and low pH*.

Discussion

Characteristics of the HT Conformers. For *cis*-PtA_2**G**$_2$ type adducts, the dominance of HT conformers over the HH form can be attributed to the better dipole (base)−dipole (base) alignment and the lower base−base steric clashes of the HT vs HH orientation. Because such interactions involve those parts of ligands close to the metal, we call these interligand interactions "first sphere−first sphere communication" (FFC). The major HT conformer for **Me$_2$DAB**-Pt**G**$_2$ adducts has the carrier-ligand NH located on the opposite side of the coordination plane from **G** O6.[31,39] The favored form cannot participate in a **G** O6 hydrogen bond, consistent with the hypothesis that carrier-ligand H-bonding is not important.[11,20,39] Positioning of the *N*-methyl substituent appears to be the key factor in making **Me$_2$DAB** a chirality-controlling chelate (**CCC**) ligand. The substituent on the N controls the positioning of the NH groups, but its bulk also controls canting direction.[31] The *S*,*R*,*R*,*S* chirality favors L canting, and the *R*,*S*,*S*,*R* chirality favors R canting (Figure 13).[28−32,38,39] This influence of the **CCC** ligand on canting has been found for all **G**'s and also for dinucleotides.[28−32,38] Because the interactions responsible involve parts of ligands close to the metal, these are examples of FFC.

Relative to the case in which the bases are both perpendicular to the coordination plane, canting will move the six-membered rings closer in to the midpoint between the N7 atoms ("6-in" form) or farther out from this midpoint ("6-out" form) (Figure 13). In typical cases, the "6-in" form is favored. The consequences of L and of R canting are different for ΔHT and ΛHT forms. In each (*S*,*R*,*R*,*S*)-**Me$_2$DAB**Pt**G**$_2$ adduct, the canting is L and we find for pH < 8 the following: the "6-in" major form is ΛHT L, and the "6-out" minor form is ΔHT L. In each (*R*,*S*,*S*,*R*)-**Me$_2$DAB**Pt**G**$_2$ adduct, the canting is R and we find for pH < 8 the following: the "6-in" major form is ΔHT R, and the "6-out" minor form is ΛHT R. It is reasonable to attribute the greater stability of the major HT form to a preferred dipole interaction between the bases because having the larger six-membered guanine rings close to each other as in the "6-in" form is not a sterically favorable situation. In minor "6-out" HT forms, **G** O6 is closer to the sterically less demanding NH part of **Me$_2$DAB** ligand, possibly allowing **G** O6−NH hydrogen bonding. Also, the bulkier six-membered rings are far from each other. These favorable FFC effects do not fully compensate for the FFC dipole effects, which appear to be less favorable in the "6-out" minor HT form, when compared to the "6-in" major HT form.

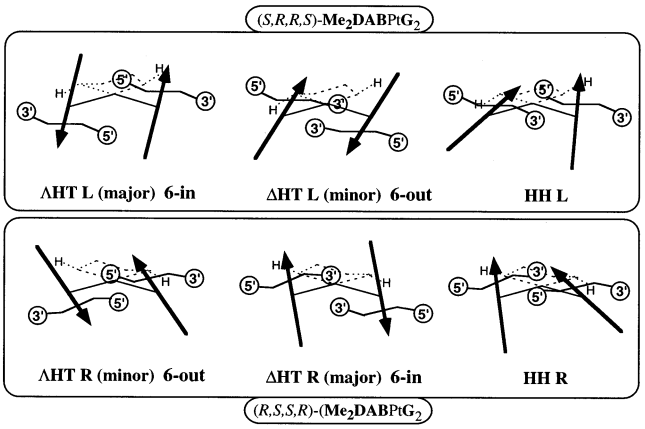

Figure 13. Sketches of the HT and HH conformers of (*S*,*R*,*R*,*S*)- and (*R*,*S*,*S*,*R*)-(**CCC**)Pt**G**$_2$ with left-handed and right-handed canting, respectively, using arrows to represent N7-bound **G** bases as shown in Figure 1. Distribution of major and minor conformers is for pH < 8. Only a small part of the **Me$_2$DAB** and **Bip** ligands shared by both is shown here for clarity. We attempt to depict the base canting fairly accurately because this feature is now well supported by the data. Circled 3′ and 5′ represent the 3′- and 5′-phosphate groups, respectively. The position is not easily fixed, as there is considerable conformational freedom in the ribose ring and the torsion angles linking the phosphate group to the nucleobase. However, the illustration is designed to convey the distinct differences in the likely positions of the 5′-phosphate relative to the 3′-phosphate group.

In addition to the direction of canting and the relative orientation of the five- and the six-membered rings, the bases in the HT forms could also differ in having a low or a high degree of canting. In the solid state, extensive structural data are available for the typical *cis*-PtA_2**G**$_2$ complexes.[42,70−80] The HT forms observed cluster into two groups differing in the direction of the cant.[10,42,76,78,80] For dynamic *cis*-PtA_2**G**$_2$ models in which **G** = nucleosides and 5′-NMP's, the ΔHT forms were observed exclusively in the solid state;[70−73,81] all of the ΔHT forms had right-handed canted bases. A high degree of canting, allowing **G** O6−NH hydrogen bonding, has been found only when the **G** derivative was not a 5′-NMP or when the base was in an oligonucleotide;[74−76,78−80,82,83] in solid-state structures of 5′-NMP complexes, the direction of canting is unfavorable for **G** O6−NH H-bonding, which is absent or weak.[14,70,73,80,81] We now have extensive evidence *in solution* that bases in retro models cant, that the degree of canting can be high or low, and that the direction of canting can allow H-bonding, even for **G** = nucleosides and NMP's.[28−32,38,39]

The H8 signal of the major HT form is downfield from the H8 signal of the minor HT form in (**CCC**)Pt$\mathbf{G}_2$ adducts.[28,30,31,39,45] The H8 shift is influenced by the positioning of the H8 atom with respect to the shielding cone of the cis **G**. This position is a consequence of two factors: the direction and the degree of canting. The canting of the two equivalent bases in the direction moving each H8 toward the cis **G** will lead to greater H8 shielding and hence an upfield H8 signal relative to the average H8 signal. This direction of canting occurs for the minor HT forms (ΔHT L and ΛHT R) (Figure 13). The interaction of the **G** H8 with the cis **G** has a small steric effect and is associated with a rather high degree of canting in X-ray data.[82] For minor HT forms, the **Me$_2$DAB** ligand should not impede base canting because the **G** O6 is closer to the small NH side of the carrier ligand (Figure 13). In contrast, for the major HT forms (ΛHT L and ΔHT R) the canting of the base that moves its H8 away from the cis **G** will lead to less H8 shielding or perhaps deshielding in the HT form[42] and hence a more downfield H8 signal. This direction of canting (i.e., the larger six-membered rings of the two cis **G**'s closer together than in the minor HT forms, Figure 13) is associated in X-ray data with a lower degree of canting.[80]

The equivalent bases in each HT form have H8 signals at shifts intermediate to those of the nonequivalent bases of the (**CCC**)Pt$\mathbf{G}_2$ HH form. The **G** base of the (**CCC**)Pt$\mathbf{G}_2$ HH form with O6 closest to the NH is canted toward the cis **G** and has a relatively upfield H8 signal (HH_u), and the base with O6 closest to the NCH_3 or NCH_2 group has a downfield H8 signal (HH_d).[28,30,31,39,45] This latter base is less canted and is probably canted away from the other **G**.

The H8 and H2 signals of hypoxanthine are inherent complementary probes for assessing conformation. We recently found that, for (**CCC**)Pt(1-Me-5′-GMP)$_2$ adducts, **G** N1−CH_3 signals follow a trend opposite to that of the H8 and H1′ signals.[39] Because the H2 atoms of hypoxanthine adducts are positioned relatively in the same place as the N1−CH_3 groups (schematically, tail of the arrow), the method of assignment of the H2 signals is similar to that for the N1−CH_3 signals (Table 2).[39]

Phosphate Group Effects on HT Conformers. We now consider the effects of the phosphate groups in **G** nucleotides. In addition to base−base and base−carrier ligand FFC effects, the favored HT form in (**CCC**)Pt$\mathbf{G}_2$ retro models with **G** = 5′-GMP can possibly be stabilized by phosphate−carrier ligand NH hydrogen bonding; we call this "first-to-second-sphere communication" (FSC). These findings and the fact that the group most likely to participate in H-bonding in the HH DNA adduct is the 5′-phosphate group[11,14,18] reveal the need to assess FSC. In the solid state, numerous examples of ΔHT complexes of 5′-GMP and several related 5′-phosphate derivatives have been found not only for Pt with various carrier ligands but also even for other metals.[42,70−82,84−87] The nucleotides in the structures have very similar relationships, with the purine bases having the same relative positions and the phosphate group always hydrogen-bonded to the cis ligand in a similar manner. This prevalence of FSC in the solid contrasts with its relative unimportance in solution.[39]

One premise of our retro-model studies is that dynamic nucleotide complexes will often have very different structures in the solid state and in solution. Also, we find that NH groups have weak (if any) interactions with the **G** O6 group in retro models.[20] Many examples of **G** O6−NH hydrogen bonds in the solid state have been reported, both before our work and afterward.[74−76,78,79] We attribute this difference between solution and solid-state results to the fact that crystals of very small molecules usually contain little or no water. The solid state could favor a hydrogen bond or even a conformer[37] that either may not be present or may be of minor importance in water. Moreover, the charged phosphate groups will be attracted to the cationic Pt center in the solid, whereas the electrostatic attraction normally will be less in water. Thus, crystallography can often provide misleading or incomplete information about interactions in aqueous solutions.

Previously we demonstrated that, in the aqueous environment where the electrostatic attraction of the amine phosphate group to the cationic Pt moiety is weak, phosphate−cis **G** N1H interactions are a key factor stabilizing the favored HT conformer. We call such interligand interactions "second-sphere communication" (SSC) because the interaction groups are at the periphery of different groups.[36,37,39] These SSC interactions are optimal at pH 6−7, conditions in which the phosphate group is deprotonated and the N1 is protonated.

The HT form favored differs for **G** = 5′-GMP (favoring ΛHT) and 3′-GMP (favoring ΔHT).[30,33−37] We have begun to understand some of the reasons for this difference.[39] The 5′-phosphate group position is different in 5′-NMP's vs 3′-

(70) Cramer, R. E.; Dahlstrom, P. L.; Seu, M. J. T.; Norton, T.; Kashiwagi, M. *Inorg. Chem.* **1980**, *19*, 148−154.
(71) Marzilli, L. G.; Chalilpoyil, P.; Chiang, C. C.; Kistenmacher, T. J. *J. Am. Chem. Soc.* **1980**, *102*, 2480−2482.
(72) Kistenmacher, T. J.; Chiang, C. C.; Chalilpoyil, P.; Marzilli, L. G. *J. Am. Chem. Soc.* **1979**, *101*, 1143−1148.
(73) Barnham, K. J.; Bauer, C. J.; Djuran, M. I.; Mazid, M. A.; Rau, T.; Sadler, P. J. *Inorg. Chem.* **1995**, *34*, 2826−2832.
(74) Lippert, B.; Raudaschl, G.; Lock, C. J. L.; Pilon, P. *Inorg. Chim. Acta* **1984**, *93*, 43−50.
(75) Schöllhorn, H.; Raudaschl-Sieber, G.; Müller, G.; Thewalt, U.; Lippert, B. *J. Am. Chem. Soc.* **1985**, *107*, 5932−5937.
(76) Grabner, S.; Plavec, J.; Bukovec, N.; Di Leo, D.; Cini, R.; Natile, G. *J. Chem. Soc., Dalton Trans.* **1998**, *9*, 1447−1451.
(77) Orbell, J. D.; Taylor, M. R.; Birch, S. L.; Lawton, S. E.; Vilkins, L. M.; Keefe, L. J. *Inorg. Chim. Acta* **1988**, *152*, 125−134.
(78) Cini, R.; Grabner, S.; Bukovec, N.; Cerasino, L.; Natile, G. *Eur. J. Inorg. Chem.* **2000**, *7*, 1601−1607.
(79) Sindellari, L.; Schöllhorn, H.; Thewalt, U.; Raudaschl-Sieber, G.; Lippert, B. *Inorg. Chim. Acta* **1990**, *168*, 27−32.
(80) Sinur, A.; Grabner, S. *Acta Crystallogr., Sect. C* **1995**, *51*, 1769−72.
(81) Gellert, R. W.; Bau, R. *J. Am. Chem. Soc.* **1975**, *97*, 7379−7380.
(82) Orbell, J. D.; Wilkoski, K.; De Castro, B.; Marzilli, L. G.; Kistenmacher, T. J. *Inorg. Chem.* **1982**, *21*, 813−821.
(83) Admiraal, G.; van der Veer, J. L.; de Graaff, R. A. G.; den Hartog, J. H. J.; Reedijk, J. *J. Am. Chem. Soc.* **1987**, *109*, 592−594.
(84) Miller, S. K.; van der Veer, D. G.; Marzilli, L. G. *J. Am. Chem. Soc.* **1985**, *107*, 1048−1055.
(85) Begum, N. S.; Poojary, M. D.; Manohar, H. *J. Chem. Soc., Dalton Trans.* **1988**, *5*, 1303−1307.
(86) Mangani, S.; Orioli, P. *J. Chem. Soc., Chem. Commun.* **1985**, *12*, 780−781.
(87) Poojary, M. D.; Hattikudur, M. *J. Chem. Soc., Chem. Commun.* **1982**, *10*, 533−534.

NMP's. In the ΛHT forms, the phosphate group is toward the cis 5′-nucleotide; in the ΔHT forms, the phosphate group is away from the cis 5′-nucleotide (Figure 13). For 3′-NMP adducts, the 3′-phosphate is close to the cis 3′-nucleotide in the ΔHT forms and away from it in the ΛHT forms (Figure 13). Thus, the relative positions of phosphate groups to the cis **G** in a HT form with a given chirality are opposite for 3′-NMP vs 5′-NMP adducts.

pH Dependence of H8 Chemical Shifts for NMP Adducts. Although the shifts of the H8 signal are useful for assessing the conformer distribution and the canting of one **G** base relative to the cis **G**, complications arise when **G** is a 5′-NMP. H8 atoms are deshielded more by a deprotonated phosphate group than by a protonated phosphate group, leading to a "wrong-way" (i.e., a downfield) shift of the H8 signal.[58] For 5′-NMP's, rotation about the glycosyl bond to form syn and anti conformers is rapid, and the H8 shifts of the various conformers will reflect the average of the syn/anti conformations of each. Between pH ∼4 and pH ∼7, 5′-phosphate deprotonation of 5′-NMP's either free or bound to Pd at the N7 position in **dien**Pd(5′-NMP) complexes (**dien** = diethylenetriamine) leads to a downfield shift of the H8 signal. The extent of this "wrong-way" shift was comparable for free 5′-AMP, 5′-GMP, and 5′-IMP (∼0.15 ppm);[58] the Pd N7-bound 5′-NMP's also showed comparable downfield shift changes (∼0.26 ppm).[58] The "wrong-way" shift on 5′-phosphate deprotonation was attributed to an increased preference of the anti conformer (the 5′-phosphate is closer to H8 in this conformer), in addition to the higher deshielding of the deprotonated phosphate group.[58] Downfield shifts of ∼0.2 ppm from pH ∼4 to pH ∼7 have also been observed for platinum adducts containing 5′-NMP's, a result consistent with the "wrong-way" shift effect of the 5′-phosphate group.[88−91] A negligible downfield shift (0.01 ppm) for the H8 signal was observed upon the 3′-phosphate deprotonation of **en**Pt(3′-GMP)$_2$;[64] however, the downfield shift of the H8 signal was significant (> 0.1 ppm) for the **en**Pt(5′-GMP)$_2$ complex.[37,64] Regardless of the syn or anti conformation of a 3′-NMP, the 3′-phosphate group cannot approach as closely to the H8 atom as the 5′-phosphate group in the anti conformation of a 5′-NMP. Thus, the result with the **en**Pt-(3′-GMP)$_2$ complex is consistent with the accepted explanation of the 5′-phosphate "wrong-way" shift effect.

Phosphate Group Effects on Nucleobase Signals in Me$_2$DAB Retro Models. We can use "wrong-way" shift effects to probe the relative position of the phosphate group to the H8 atom. In the HH form, the HH$_d$ signal for the (*S*,*R*,*R*,*S*)- and (*R*,*S*,*S*,*R*)-**Me$_2$DAB**Pt(5′-NMP)$_2$ adducts always shifted ∼0.25 ppm downfield upon phosphate deprotonation (Tables 1 and 2, Supporting Information). However, a negligible shift (0.02 ppm) occurred for the HH$_d$ signal of (*S*,*R*,*R*,*S*)-**Me$_2$DAB**Pt(3′-NMP)$_2$ adducts upon phosphate deprotonation (Tables 1 and 2, Supporting Information). We use the H2 shifts to understand more about the H8 shifts. Although the HH$_c$ and HH$_n$ signals were very small for some adducts, they were helpful for assessing canting in the HH form. For example, for (*S*,*R*,*R*,*S*)- and (*R*,*S*,*S*,*R*)-**Me$_2$DAB**-Pt(5′-IMP)$_2$ adducts, the H2 partners (HH$_c$ signals) to the HH$_d$ signals did not shift. If the HH$_d$ shift change (∼0.25 ppm) for these two complexes were due to a change in canting, it would have been also reflected on the HH$_c$ signals and would have led to an upfield shift for this signal. For the 5′-NMP complexes, the HH$_d$ signal arises from that **G** having a 5′-phosphate group possibly positioned to form an H-bond with the cis NH of the carrier ligand. This positioning and the alignment of the **G** base produce a short distance between this 5′-phosphate group and the H8 atom. Our molecular modeling calculations (data not shown) support this suggestion. Thus, a "wrong-way" shift upon phosphate deprotonation can explain the shift change for HH$_d$.

The changes in shift upon phosphate deprotonation of the ΔHT conformer were also analyzed. The ΔHT H8 signals of (*R*,*S*,*S*,*R*)-**Me$_2$DAB**Pt(5′-GMP)$_2$ and (*R*,*S*,*S*,*R*)-**Me$_2$DAB**-Pt(5′-IMP)$_2$ adducts shifted by ∼0.15−0.20 ppm; the ΔHT H2 signal of the 5′-IMP adduct shifted slightly upfield (0.04 ppm) (Figure 11 and Supporting Information). Plastic models reveal that the 5′-phosphate groups can occupy positions that permit H-bonding to NH groups of the carrier ligands, consistent with the ΔHT model illustrated in Figure 13. This H-bonding places the H8 atoms close to these phosphate groups; thus, the H8 signal is downfield shifted by phosphate deprotonation. Of particular note, this H-bonded model has a structure similar to that of the ΔHT form observed for **en**Pt(5′-GMP)$_2$ in the solid state.[73]

For (*S*,*R*,*R*,*S*)-**Me$_2$DAB**Pt(3′-GMP)$_2$ and (*S*,*R*,*R*,*S*)-**Me$_2$DAB**-Pt(3′-IMP)$_2$ also, the ΔHT H8 signals shifted significantly downfield (Tables 1 and 2). For the latter, the ΔHT H2 signal shifted slightly upfield. On the other hand, only a slight downfield shift was observed for the ΔHT H8 signals of (*R*,*S*,*S*,*R*)-**Me$_2$DAB**Pt(3′-GMP)$_2$ and the respective 3′-IMP complexes. Because the 3′-phosphate groups are always far from the H8 atoms, we believe that the ΔHT H8 downfield shift for (*S*,*R*,*R*,*S*)-**Me$_2$DAB**Pt(3′-GMP)$_2$ and the respective 3′-IMP adduct is not caused by the "wrong-way" deshielding effect. Models reveal that SSC can alter canting, and we attribute the downfield shift of the H8 signal of these ΔHT conformers to a decrease in canting, moving the H8 away from the cis base. In summary, our results clearly show that the "wrong-way" shift occurs only for the 5′-NMP complexes and only when the phosphate group is close to H8.

Influence of N1H Deprotonation on the H8 and H2 Shifts. One goal of this study is to assess the influence on conformer distribution of phosphate position when the N1H is deprotonated. Near the end of the Discussion, we summarize arguments that the **G** 2-NH$_2$ group has little influence on properties. Upon N1H deprotonation, upfield shifts are usually observed for the H8 signals; these upfield shifts are dramatic (∼0.3−0.6 ppm) for the minor "6-out" conformers that allow **G** O6−(NH)**CCC** H-bonding. Stronger H-bonding

(88) Dijt, F. J.; Canters, G. W.; den Hartog, J. H. J.; Marcelis, A. T. M.; Reedijk, J. *J. Am. Chem. Soc.* **1984**, *106*, 3644−3647.
(89) Inagaki, K.; Dijt, F. J.; Lempers, E. L. M.; Reedijk, J. *Inorg. Chem.* **1988**, *27*, 382−387.
(90) Bloemink, M. J.; Dorenbos, J. P.; Heetebrij, R. J.; Keppler, B. K.; Reedijk, J.; Zahn, H. *Inorg. Chem.* **1994**, *33*, 1127−1132.
(91) Bloemink, M. J.; Engelking, H.; Karentzopoulos, S.; Krebs, B.; Reedijk, J. *Inorg. Chem.* **1996**, *35*, 619−627.

could cause greater canting, which will place the H8 atom closer to the shielding cone of the cis **G**.[38] Two factors can affect the upfield shifts of the H8 and H2 signals at high pH: the inductive effect caused by deprotonation of the N1H (especially on the H2) neighboring; the effect of the cis **G** when N1H deprotonation leads to changes in the canting degree. For (*S,R,R,S*)-**Me$_2$DAB**Pt(3′-IMP)$_2$ at pH 9.8, the "6-out" ΔHT H8 signal shifted ∼0.6 ppm upfield, while the ΔHT H2 signal did not shift; however, the "6-in" ΛHT H8 and H2 signals shifted by ∼0.1 ppm. The similar upfield shift of the "6-in" ΛHT H8 and H2 signals is most likely the result of the inductive effect caused by N1H deprotonation. For the "6-out" ΔHT H8 signal, the change in **G** base canting to allow **G** O6−(NH)**Me$_2$DAB** H-bonding is substantially responsible for the ∼0.6 ppm upfield shift. The absence of a ΔHT H2 shift is most likely due to the net result of two effects: (i) The change in **G** base canting causes the ΔHT H2 signal to shift downfield. (ii) An inductive effect of N1H deprotonation causes a ΔHT H2 upfield shift of ∼0.1 ppm.

For (*S,R,R,S*)-**Me$_2$DAB**Pt(5′-IMP)$_2$, the "6-out" ΔHT H8 and H2 signals shifted upfield by 0.3 and 0.04 ppm upon N1H deprotonation, respectively. The shift of the ΔHT H8 signal is due to a change in **G** base canting, while the shift of the ΔHT H2 signal is the net shift of the inductive effect and change in **G** base canting (as discussed above). On the other hand, the similar (0.11−0.15 ppm) upfield shifts of the "6-in" ΛHT H8 and H2 signals at high pH are most likely caused primarily by the inductive effect following N1H deprotonation. This analysis can be applied for the rest of adducts (Tables 1 and 2). We conclude that, for the major "6-in" conformer of **Me$_2$DAB**Pt(3′-IMP)$_2$ and **Me$_2$DAB**Pt-(5′-IMP)$_2$, the similarity in upfield shifts (∼0.10−0.15 ppm) of the H8 and H2 signals is most likely caused by the inductive effect of N1H deprotonation. However, for the minor "6-out" conformer the large H8 upfield shifts (0.3−0.6 ppm) and the very slight (0.04 ppm) or negligible upfield shift of H2 signals reflect the net effects of N1H deprotonation (upfield) and of the change of **G** base canting (downfield).

Dependence of Conformer Distribution on pH. 3′-GMP and 3′-IMP Adducts. The (*S,R,R,S*)-**Me$_2$DAB** ligand favors L canting and the "6-in" ΛHT conformation for (*S,R,R,S*)-**Me$_2$DAB**Pt**G**$_2$ complexes. For both **G** = 3′-GMP and 3′-IMP, the changes in intensities and chemical shifts of the H8 signals were similar throughout the pH titration. (NH)-**Me$_2$DAB**−cis **G** O6 H-bonding could contribute to the stability of the minor form, but this interaction would be at best weak. Also, SSC involving the 3′-PO$_4$ group stabilizes the minor ΔHT conformer. At pH ∼3, SSC is weak because the phosphate group is protonated. Thus, the carrier-ligand effect favoring L canting and the "6-in" ΛHT conformer prevails. At pH ∼7, the abundance of the ΔHT conformer increases, most likely because of the enhancement of the phosphate−cis **G** interactions when the phosphate group is deprotonated. In adducts of 3′-nucleotides, L canting does not allow such favorable SSC as does R canting. Thus, the ΔHT L form remains at low abundance, not only at low pH but also at pH 7.

Upon deprotonation at higher pH of the guanine six-membered ring N1H of (*S,R,R,S*)-**Me$_2$DAB**Pt**G**$_2$, the "6-out" ΔHT conformer became more favored. This relative increase in stability can arise from two causes: reduction of electrostatic repulsion between the two negatively charged N1 atoms, which in an L-canted "6-out" ΔHT conformer are placed farther apart than in the L-canted "6-in" ΛHT conformer; (ii) enhancement of the **G** O6−(NH)**Me$_2$DAB** hydrogen bonding as a result of the increase in capacity of the **G** O6 as a hydrogen bond acceptor. In the "6-out" form, the O6 is positioned to form such an H-bond.

For (*R,S,S,R*)-**Me$_2$DAB**Pt**G**$_2$ complexes the (*R,S,S,R*)-**Me$_2$DAB** ligand favors R canting, for which the "6-in" form is the ΔHT conformer. For both **G** = 3′-GMP and 3′-IMP, the changes in intensities and chemical shifts of the H8 signals were similar throughout the pH titration. The "6-in" ΔHT conformer is favored by both the dipole (base)−dipole (base) alignment and SSC. Phosphate deprotonation enhances the latter interaction, which leads to a highly dominant ΔHT conformer at pH ∼7. The "6-out" R-canted ΛHT conformer has an unfavorable dipole alignment but still has the possibility of forming a **G** O6−(NH)**Me$_2$DAB** hydrogen bond. At pH ∼10, the N1H deprotonation eliminates the SSC PO$_4$−cis **G** N1H interactions and creates electrostatic repulsion, thus destabilizing the "6-in" ΔHT conformer. On the other hand, the "6-out" ΛHT conformer has lower electrostatic repulsion because the negatively charged N1 guanine atoms are farther apart, and this conformer can have better hydrogen bonding of **G** O6 with the NH of **Me$_2$DAB**. Therefore, the "6-out" ΛHT conformer becomes dominant at high pH.

Dependence of Conformer Distribution on pH. 5′-GMP and 5′-IMP Adducts. Both the *S,R,R,S* carrier-ligand chirality and the 5′-phosphate group favor the L-canted "6-in" ΛHT conformer for (*S,R,R,S*)-**Me$_2$DAB**Pt(5′-NMP)$_2$ adducts. At low pH, the ΛHT conformer is stabilized by the favorable alignment of the base dipoles and favorable SSC PO$_4$−cis **G** interactions; the latter interactions are enhanced when the 5′-phosphate groups are deprotonated, thus leading to a higher abundance of the major "6-in" ΛHT conformer. The unfavorable alignment of **G** bases in the "6-out" ΔHT conformer makes this form less abundant; however, as discussed above, release of electrostatic repulsion between negatively charged N1 atoms and **G** O6−(NH)**Me$_2$DAB** hydrogen bonding greatly favor the "6-out" HT conformer at pH ∼10. A noteworthy observation is that higher pH (>10) is needed for (*S,R,R,S*)-**Me$_2$DAB**Pt**G**$_2$ (**G** = 5′-GMP and 5′-IMP) complexes to reach full N1H deprotonation compared to their respective 3′-GMP and 3′-IMP adducts. This observation provides evidence for N1H sites with lower acidity in the 5′-GMP or 5′-IMP adducts. This difference between 5′-NMP and 3′-NMP adducts was observed for the free NMP's.[62]

(*R,S,S,R*)-**Me$_2$DAB**Pt(5′-GMP)$_2$ and (*R,S,S,R*)-**Me$_2$DAB**-Pt(5′-IMP)$_2$ respond similarly to pH changes. For both, the intensity of the H8 NMR signals did not change significantly,

and no inversion of the ΔHT/ΛHT ratio occurred as the pH was increased to ~10 (Figure 12 and Supporting Information). The (*R*,*S*,*S*,*R*)-**Me$_2$DAB** ligand stabilizes the R-canted "6-in" ΔHT conformer. Because for 5′-nucleotides the minor "6-out" ΛHT conformer is stabilized by SSC, the 5′-phosphate group deprotonation will further stabilize this form. It should be noted that interaction of the 5′-phosphate group with an **Me$_2$DAB** NH group (FSC) is not important; otherwise, the ΔHT conformer would have increased in abundance from pH ~3 to pH ~7 because this conformer allows such H-bonding (see Figure 13). These results indicate that in the ΛHT form SSC is more important than FSC.

At pH ~10, we would have expected **G** O6−NH hydrogen bonding to dominate the interactions and lead to a favored ΛHT conformer. However, these (*R*,*S*,*S*,*R*)-**Me$_2$DAB**Pt(5′-NMP)$_2$ adducts are anomalous, and the ΔHT form continues to dominate. A combination of three factors might explain this finding. First, just as the proximity of the 5′-phosphate group to the cis **G** N1H is favorable for SSC, this proximity could be highly unfavorable when N1H is deprotonated and carries a 1− charge. Second, the movement of the 5′-phosphate group away from the negative N1 would postion it for favorable FSC interactions which are possible in the ΛHT form. Finally, the H8 signals remain relatively downfield in the ΔHT form; this downfield shift position could indicate a lesser degree of canting. In this case, N1-to-N1 distances are longer, minimizing the repulsive N1−N1 effect.

Influence of the G 2-NH$_2$ Group on Conformer Properties. All the studies suggest that the **G** N1H group is key in SSC for *cis*-PtA$_2$(GMP)$_2$.[30,33,34,36,37,39] Experimental results involving N1H deprotonation suggested that the **G** 2-NH$_2$ was not a significant hydrogen-bond donor contributing to SSC.[33,36,37] However, N1H deprotonation could weaken the 2-NH$_2$ to phosphate hydrogen bonding both electrostatically and inductively. Thus, replacing the 2-NH$_2$ group with an H2 as in the hypoxanthine base of IMP eliminates any possible effect of the 2-NH$_2$ group. In the past, a few Pt−IMP complexes were studied.[36,37,92] Two of these complexes were fluxional.[37,92] First, *cis*-Pt(NH$_3$)$_2$(5′-IMP)$_2$ showed only one H8 and one H2 NMR signal, reflecting signals of conformers in fast interconversion.[92] Second, the *cis*-Pt(NH$_3$)$_2$(3′-IMP)$_2$ adduct was studied by CD spectroscopy at different pH values.[37] At pH ~3, the CD spectrum exhibited features characteristic of the ΔHT conformer; these features increased in intensity at pH ~7, indicating the enhancement of the ΔHT abundance conformer at this pH. At pH ~11, the CD features inverted, indicating the dominance of the ΛHT conformer at this high pH. Because the *cis*-Pt(NH$_3$)$_2$(IMP)$_2$ adducts are highly dynamic, their NMR spectra are uninformative for assessing factors stabilizing the HT and HH conformers. Later, **Me$_2$ppz**Pt(5′-IMP)$_2$ and **Me$_2$ppz**Pt(3′-IMP)$_2$ retro models were studied by NMR and CD spectroscopy.[36] Conformer distribution was essentially similar to the respective guanine adducts at pH ~3, ~7, and ~10, suggesting that the **G** 2-NH$_2$ group has no role. However, relative to GMP analogues, **Me$_2$ppz**Pt(5′-IMP)$_2$ and **Me$_2$ppz**Pt(3′-IMP)$_2$ adducts were changed in two ways simultaneously (absence of 2-NH$_2$ groups, which might participate in SSC, and lack of carrier ligand NH groups that might participate in FSC). Thus, conclusions about the H-bonding of the **G** 2-NH$_2$ group required confirmation by the studies reported here.

(92) Marcelis, A. T. M.; Erkelens, C.; Reedijk, J. *Inorg. Chim. Acta* **1984**, *91*, 129−135.

Table 4. Interligand Interactions Contributing to the Stability of HT Conformers of (**CCC**)Pt(GMP)$_2$ Adducts at Different pH Values

			pH		
canting	**G**	conformation	3	7	10
left-handed	3′-GMP	ΛHT	*a*	*a*	*a*
		ΔHT		*b*	*d*
	5′-GMP	ΛHT	*a*	*a, b*	*a*
		ΔHT			*d*
right-handed	3′-GMP	ΔHT	*a*	*a, b*	*a*
		ΛHT			*d*
	5′-GMP	ΔHT	*a*	*a, c*	*a, c*
		ΛHT		*b*	

[a] Dipole (base)−dipole (base) alignment (FFC). (When a second interaction is listed, the more important interaction is first.) [b] PO$_4$−cis **G** interactions (SSC). [c] PO$_4$−cis amine interactions (FSC). [d] Lower electrostatic repulsion caused by the greater distance between the negatively charged N1 atoms (FFC) and/or **G** O6−cis amine hydrogen bonding (FFC).

For **Me$_2$DAB**Pt(3′-NMP)$_2$ adducts the conformer distribution and the abundance of the ΔHT conformer were very similar throughout the entire pH range for either **Me$_2$DAB** chirality (Table 3). Because of these similarities, we conclude that the 2-NH$_2$ group in 3′-GMP adducts is not important in influencing stability of the conformers. For 3′-NMP adducts, the key structural element in the nucleobase for SSC is the N1H.

Likewise, the conformer distribution for **Me$_2$DAB**Pt(5′-NMP)$_2$ adducts in the pH range ~3 to ~10 revealed that the (*S*,*R*,*R*,*S*)-**Me$_2$DAB**Pt(5′-NMP)$_2$ distributions were very similar (Table 3). Except for the ΛHT conformer, this similar distribution applies to the (*R*,*S*,*S*,*R*)-**Me$_2$DAB**Pt(5′-NMP)$_2$ adducts. The 5′-GMP adduct had an ~8% more abundant ΛHT conformer than the 5′-IMP adduct. Except for this case in which the 2-NH$_2$ group may have a small role, these findings indicate that the N1H plays the key role in SSC for 5′-GMP adducts.[30,33,36,37,39]

Factors Stabilizing the HH Conformer for Me$_2$DAB-PtG$_2$ Adducts. The HH form of **Me$_2$DAB**Pt**G**$_2$ adducts has a higher abundance for **G** = 5′-NMP's than for **G** = 3′-NMP's. Furthermore, the finding that the HH conformer was also abundant in the case of **Me$_2$ppz**Pt(5′-GMP)$_2$[35,36] and the results reported in this study reinforce the general finding that the 5′- phosphate group stabilizes the HH conformer. The information in this study does not illuminate this issue beyond the concepts presented in previous studies.[36,39]

Retro-Models Comparison. On the basis of the new and previous results,[28,30,31,39,45] the interactions contributing to the stability of various conformers of (**CCC**)Pt**G**$_2$ complexes at different pH values are summarized in Table 4 and illustrated schematically in Figure 13. In order of apparent relative importance, the interactions are as follows: (a) dipole (base)−dipole (base) interaction (stronger in the "6-in" HT conformer and most clear below pH 8); (b) SSC (phosphate−cis **G** N1H interactions) contributing at low and neutral pH

(does not exist at high pH); (c) release of electrostatic repulsion between the negatively charged N1 guanine atoms in the "6-out" HT form (relevant at high pH); (d) release of electrostatic repulsion between the negatively charged N1 atom and the 5′-phosphate group, most important in favoring the ΔHT form (relevant at high pH); (e) amine NH hydrogen-bonding interactions with the O6 of both deprotonated **G**'s in the "6-out" HT form and of one deprotonated **G** of the HH form (contributing only at high pH because N1H deprotonation increases the capacity of the **G** O6 as an H-bond acceptor); (f) 5′-phosphate−cis amine NH hydrogen-bonding interactions (most relevant at neutral and basic pH); (g) amine NH hydrogen-bonding interactions with the O6 of both **G**'s of the "6-out" HT form and of one **G** in the HH form (below pH 8, where **G** N1H is not deprotonated).

Conclusion. Each **Me$_2$DAB**Pt**G**$_2$ retro model adduct at pH ∼7 has a major HT form with the six-membered base rings close to each other ("6-in") and a minor HT form with the rings farther apart ("6-out"). In the minor "6-out" HT form, the separation of the larger six-membered rings could be sterically favorable. Also, **G** O6 is closer to the sterically less demanding NH part of **Me$_2$DAB** ligand, possibly allowing **G** O6−NH hydrogen bonding. These favorable FFC effects in the minor "6-out" HT form do not fully compensate for possibly highly favorable strong dipole effects in the major "6-in" HT form. Second-sphere communication (SSC) between peripheral groups also affects distribution. Phosphate−N1H cis **G** interactions favor ΛHT forms in 5′-GMP and 5′-IMP complexes and ΔHT forms in 3′-GMP and 3′-IMP complexes. When SSC and FFC favor the same HT conformer, it is present at > 90% abundance. In six adducts [4 (*S*,*R*,*R*,*S*)-**Me$_2$DAB**Pt**G**$_2$; (*R*,*S*,*S*,*R*)-**Me$_2$DAB**Pt**G**$_2$ with 3′-GMP and with 3′-IMP], the minor "6-out" HT form at pH ∼7 becomes the major form at pH ∼10 (where **G** N1H is deprotonated) because the larger distance between the negatively charged N1 atoms decreases electrostatic repulsion and possibly because the **G** O6−(NH)**Me$_2$DAB** hydrogen bond is favored by N1H deprotonation. At pH ∼10, phosphate-negative N1 repulsion is an unfavorable SSC term. This factor disfavors the ΛHT R form of two (*R*,*S*,*S*,*R*)-**Me$_2$DAB**Pt**G**$_2$ (**G** = 5′-GMP and 5′-IMP) adducts to such an extent that the "6-in" ΔHT R form remains dominant even at pH ∼10.

A comparison of the results for the GMP and IMP adducts showed without doubt that the role of the **G** 2-NH_2 group in SSC is *minimal* and that N1H is the key factor. This result is consistent with the recent study of the (**CCC**)Pt(1-Me-5′-GMP)$_2$ and **Me$_2$ppz**Pt(1-Me-5′-GMP)$_2$ complexes,[36,39] in which we showed that the presence of a N1 methyl group destabilizes the ΛHT conformer by eliminating SSC and leaves the 5′-phosphate free to enhance its effect favoring the HH conformer, leading to a highly abundant HH conformer. In addition, for **Me$_2$DAB**Pt(IMP)$_2$ adducts, the H2 signals served as an additional probe to determine structural features of adducts. Results supported our previous findings[39] about the head/tail relationship of H8 atoms (head of arrow) and others located on the opposite side of the base (tail of arrow) (e.g., N1−CH_3 in 1-Me-5′-GMP or H2 in IMP).

Another important feature of these results is the striking similarity of **Me$_2$DAB**Pt**G**$_2$ adducts and their respective **Bip**Pt**G**$_2$ adducts[30] at low and neutral pH values. As we discussed earlier, the dynamic properties are very different. These data confirm the retro-model design focusing on destabilizing the transition state without altering the ground state. The results suggest that wagging of the base (i.e., fluctuation of the canting angle about an average angle) is either not large or else occurs to the same extent for adducts with either of these two ligands.

Finally, our results provided clear evidence for the importance of FFC and SSC and the inconsequential influence of FSC on the properties and conformer distribution of all **Me$_2$DAB**Pt**G**$_2$ adducts. It is quite striking that the role of hydrogen bonding of the amine NH group at neutral pH in solution appears to be relatively minimal. Studies involving the **Me$_2$ppz**Pt retro models and adducts with larger DNA fragments[48] also suggest a minimal role for amine NH H-bonding. This view is contrary to long-held beliefs, and additional studies are needed before this conclusion will be widely adopted. We have made an initial attempt to separate factors influencing H8 shifts, particularly the "wrong-way" shift effect of the phosphate group. However, studies of models with only one **G** are needed to assess fully such factors.

Acknowledgment. This work was supported by NIH Grant GM 29222 (to L.G.M.) and NATO CRG 950376 (to L.G.M. and G.N.) and by the MURST (Contribution 40%), CNR, and EC (COST Chemistry project D20/003/2000) (to G.N.).

Supporting Information Available: H8 and H2 regions of ^{1}H NMR pH titration spectra of (*S*,*R*,*R*,*S*)-**Me$_2$DAB**Pt(5′-IMP)$_2$ and (*R*,*S*,*S*,*R*)-**Me$_2$DAB**Pt(5′-IMP)$_2$; shift (ppm) vs pH profile for the H8 signals of the various **Me$_2$DAB**Pt**G**$_2$ complexes and conformer distribution vs pH of various adducts. This material is available free of charge via the Internet at http://pubs.acs.org.

IC011115M